

Saddle-shaped dioxo-ruthenium(vi) and -osmium(vi) 2,3,5,7,8,10,12,13,15,17,18,20-dodecaphenylporphyrin (H₂dpp) complexes. Synthesis, spectral characterisation and alkene oxidation by [Ru^{VI}(dpp)O₂][†]

Chun-Jing Liu,^a Wing-Yiu Yu,^a Shie-Ming Peng,^b Thomas C. W. Mak^c and Chi-Ming Che^{*a}

^a Department of Chemistry, The University of Hong Kong, Pokfulam Road, Hong Kong

^b Department of Chemistry, National Taiwan University, Taipei, Taiwan

^c Department of Chemistry, The Chinese University of Hong Kong, Shatin, Hong Kong

An improved procedure for the preparation of the saddle-distorted porphyrin 2,3,5,7,8,10,12,13,15,17,18,20-dodecaphenylporphyrin (H₂dpp) (yield = 75%) based on the Suzuki cross-coupling reaction between phenylboronic acid PhB(OH)₂ and [2,3,7,8,12,13,17,18-octabromo-5,10,15,20-tetraphenylporphyrin] has been developed. X-Ray diffraction studies of [M^{II}(dpp)(CO)(py)] (M = Ru **1** or Os **3**) showed that **1** and **3** are isostructural, and the porphyrin macrocycles exhibit severe out-of-plane saddle and ruffle distortions. In both **1** and **3** the pyrrole rings are alternately tilted up and down with respect to the least-squares plane of the 25-atom porphyrin core, and the pyrrole carbons experience an average displacement of 0.769 Å from the least-squares plane compared to 0.78 Å for free H₂dpp, whereas the Ru and Os atoms are displaced by 0.1006 and 0.0792 Å from the 25-atom porphyrin core respectively. The complex [Ru^{VI}(dpp)O₂] **2**, prepared by *m*-chloroperoxybenzoic acid oxidation, is an active oxidant for alkene epoxidations. In CH₂Cl₂ [containing 2%(w/w) pyrazole], styrene, norbornene and *cis*-stilbene were oxidised selectively to their respective epoxides in excellent yield. Complete stereoretention was observed for the oxidation of *cis*-stilbene, however oxidation of *cis*-β-methylstyrene afforded significant amounts of *trans*-epoxide suggesting that a carboradical mechanism is operative. The crystal structure of the complex [Ru^{IV}(dpp)(pz)₂] (**5**), the product of the stoichiometric alkene oxidations, was determined. Magnetic susceptibility measurement ($\mu_{\text{eff}} = 3.24 \mu_{\text{B}}$) suggests the formulation of Ru^{IV} with two unpaired electrons in its electronic ground state. The Ru–N (pz) bond distances are 2.022(13) and 2.083(12) Å. The reactions of **2** with alkenes in CH₂Cl₂ (with 2% Hpz) follow second-order kinetics: rate = $k_1[\mathbf{2}][\text{alkene}]$. For norbornene and styrene, the second-order rate constants, k_1 , in CH₂Cl₂ at 25.9 °C are $(3.79 \pm 0.04) \times 10^{-3}$ and $(4.78 \pm 0.09) \times 10^{-3} \text{ dm}^3 \text{ mol}^{-1} \text{ s}^{-1}$ respectively.

The role of non-planar conformation in modifying the biological properties and functions of some metalloporphyrins has recently come under rigorous investigations.¹ Out-of-plane distortion is observed in the crystal structures of the bacteriochlorophylls in the photosynthetic reaction centres of *Rhodospseudomonas viridis*² and the light-harvesting antenna bacteriochlorophyll *a* of *Prosthecochloris aestuarii*.³ Variations in the extent of the distortion have been proposed as a possible reason for the unidirectionality of electron transfer.⁴ On the other hand, the steric congestion among the peripheral substituents in some synthetic polyhalogenated porphyrins such as octa-β-halogenotetrakis(pentafluorophenyl)porphyrins (X = Cl or Br) has created an out-of-plane distortion of the porphyrin ligands, which is proposed to play a crucial role in enhancing the catalytic activities of the iron(III) complexes by lowering their oxidation potentials.⁵ In this respect, we are interested to examine how the reactivities/catalytic activities of ruthenium/osmium complexes could be influenced by the conformational distortion of the porphyrin macrocycles.⁶ Here we report the first synthesis and characterisation of the saddle-distorted dioxo-ruthenium(vi) and -osmium(vi) complexes of 2,3,5,7,8,10,12,13,15,17,18,20-dodecaphenylporphyrin (H₂dpp), and the

reactivities, as well as the catalytic activities, of the dioxo-ruthenium(vi) complex towards alkene oxidations.

Experimental

Materials

All solvents were purified by the standard procedures prior to use. Benzaldehyde, *tert*-butylamine, propionic acid and pyrrole were either distilled or purified by standard methods before use. Bromine and *m*-chloroperoxybenzoic acid (Merck), palladium(II) chloride, dodecacarbonyltriruthenium and dodecacarbonyltriosmium (Aldrich) were used as received. Tetrakis(triphenylphosphine)palladium(0) was prepared according to the reported procedure.⁷ 2,3,7,8,12,13,17,18-Octabromo-5,10,15,20-tetraphenylporphyrin, [H₂obtp], was obtained by bromination of [Cu^{II}(tpp)]⁸ following the procedures described by Bhyrappa and Krishnan.⁹

Physical measurements

The UV/VIS spectra were acquired on a Perkin-Elmer Lambda 19 spectrophotometer and infrared spectra on a Shimadzu IR-470 spectrophotometer. Cyclic voltammograms were recorded on a Princeton Applied Research model 273 potentiostat using a glassy carbon electrode and Ag–AgNO₃ (0.1 mol dm⁻³ in MeCN) as the reference electrode. Gas chromatography was performed on a Hewlett-Packard 5890 Series II gas chromatograph equipped with a SPB-5 capillary column (30 m) using nitrogen as the carrier gas, a flame ionisation detector and a 3396 Series II integrator. The ¹H and ¹³C NMR spectra were

[†] Supplementary data available: rate constant concentration dependencies, cyclic voltammograms. For direct electronic access see <http://www.rsc.org/suppdata/dt/1998/1805/>, otherwise available from BLDSC (No. SUP 57369, 7 pp.) or the RSC Library. See Instructions for Authors, 1998, Issue 1 (<http://www.rsc.org/dalton>).

Non-SI units employed: $\mu_{\text{B}} \approx 9.27 \times 10^{-24} \text{ J T}^{-1}$, atm = 101 325 Pa, cal = 4.184 J.

recorded on Bruker 300 and 500 NMR spectrometers. All the chemical shifts are given in ppm vs. SiMe₄. Elemental analyses were performed by Butterworth Co. Ltd., UK.

Synthesis of 2,3,5,7,8,10,12,13,15,18,20-dodecaphenylporphyrin (H₂dpp) by Suzuki cross-coupling reaction

A Teflon-stoppered flask (2 l) was charged with H₂obtp (5.7 g, 4.58 mmol), [Pd(PPh₃)₄] (800 mg, 0.69 mmol), toluene (1.3 l), dry K₂CO₃ (25.3 g, 183.2 mmol) and phenylboronic acid PhB(OH)₂ (11.17 g, 91.76 mmol). The green suspension was heated at 98 °C under nitrogen for 7 d. After cooling to room temperature the mixture was diluted with dichloromethane (1.3 l) and washed with 4% sodium hydrogencarbonate solution (3 × 600 cm³). The organic layer was then dried (Na₂SO₄) and evaporated to dryness by rotary evaporation to afford the crude product, which was purified by chromatography with a silica gel column using chloroform as the eluent. The slowest-moving green band was collected; after solvent evaporation H₂dpp was isolated as a green solid. The compound was further recrystallised from CH₂Cl₂-EtOH (1:2) to afford a green crystalline solid. Yield: 75%. ¹H NMR (300 MHz, CDCl₃): δ 7.58 (d, *J* = 6.76 Hz, 8 H) and 6.72 (m, 52 H). ¹³C NMR (75.6 MHz, CD₂Cl₂): δ 125.1, 125.7, 126.1, 126.8, 131.4, 136.6 and 138.4. FAB mass spectrum: *m/z* 1224 (*M*⁺ + 2) (Found: C, 89.46; H, 4.84; N, 4.61. Calc. for C₉₂H₆₂N₄: C, 90.34; H, 5.07; N, 4.58%).

Syntheses of ruthenium complexes

[Ru^{II}(dpp)(CO)(py)] 1. The compound H₂dpp (200 mg, 0.164 mmol) was refluxed with [Ru₃(CO)₁₂] (200 mg, 0.313 mmol) in toluene (120 cm³) under nitrogen for 4 h. The resulting red solution was evaporated at reduced pressure to dryness. The residue was then chromatographed on a basic alumina column using dichloromethane as the eluent. The second brick red band was collected. Upon addition of methanol (20 cm³), the solution was concentrated until the [Ru^{II}(dpp)(CO)(MeOH)] complex started to precipitate as a red solid. The compound was recrystallised in pyridine-dichloromethane-benzene (6:3:1, 10 cm³), and **1** was obtained as dark purple crystals. Yield ≈50% based on H₂dpp. IR(KBr): ν_{C=O} 1934 cm⁻¹. ¹H NMR (500 MHz, CD₂Cl₂): δ 3.08 (d, *J* = 6.77, 2 H), 5.77 (t, *J* = 7.02, 3 H), 6.36 (d, *J* = 7.44, 8 H), 6.50 (t, *J* = 7.2, 4 H), 6.53 (t, *J* = 1.82, 8 H), 6.59 (m, 32 H), 7.18 (d, *J* = 7.15, 4 H) and 7.38 (d, *J* = 6.71 Hz, 4 H). ¹³C NMR (75.6 MHz, CD₂Cl₂): δ 120.6, 122.8, 123.8, 124.7, 124.9, 125.0, 125.2, 125.7, 130.2, 130.7, 135.4, 135.5, 137.1, 138.4, 143.9, 144.3 and 144.8. FAB mass spectrum: 1428 (*M*⁺), 1351 (*M*⁺ - py), 1323 and 1321 (*M*⁺ - py - CO) (Found: C, 82.97; H, 4.49; N, 4.48. Calc. for C₉₈H₆₅N₅ORu·2C₆H₆: C, 83.56; H, 4.5; N, 4.29%).

[Ru^{VI}(dpp)O₂] 2. The complex [Ru^{II}(dpp)(CO)(MeOH)] (50 mg, 0.038 mmol) was completely dissolved in dichloromethane-chloroform (1:1, 15 cm³). *m*-Chloroperoxybenzoic acid (200 mg, 0.116 mmol) and absolute ethanol (5 cm³) were added sequentially, and stirring was continued for 5 min. The reaction mixture was then poured into methanol (50 cm³) with stirring, and the yellowish brown complex **2** gradually precipitated. The solid was then collected on a frit, washed with dry methanol and dried *in vacuo*. Yield: 75%. IR(KBr): ν_{Ru=O} 818, 1012 cm⁻¹ (oxidation state marker band). ¹H NMR (300 MHz, CDCl₃, SiMe₄): δ 6.68 (m, 52 H) and 7.45 (d, *J* = 7.0 Hz, 8 H). FAB mass spectrum: 1354 (*M*⁺) (Found: C, 80.9; H, 4.19; N, 4.04. Calc. for C₉₂H₆₀N₄O₂Ru: C, 81.5; H, 4.43; N, 4.13%).

Syntheses of osmium complexes

[Os^{II}(dpp)(CO)(py)] 3. A mixture of [Os₃(CO)₁₂] (200 mg, 0.221 mmol) and H₂dpp (200 mg, 0.164 mmol) in degassed diethylene glycol monoethyl ether (60 cm³) was heated at reflux for 1.5 h. The resulting red solution was diluted with benzene

(50 cm³) after cooling to room temperature, and then poured into brine (200 cm³) and extracted with benzene (3 × 100 cm³). The combined organic extracts were washed with water (3 × 50 cm³) and dried over Na₂SO₄, and then evaporated to dryness. The residue was redissolved in dichloromethane (15 cm³), and chromatographed on a basic alumina column using dichloromethane as the eluent. The leading purple band was collected and evaporated to dryness to afford dark red [Os^{II}(dpp)(CO)(MeOH)]. The solid was redissolved in pyridine-dichloromethane-ethanol (6:3:1, 10 cm³) to yield complex **3** as dark purple crystals. Yield: 45% based on H₂dpp. IR(KBr) ν_{C=O} 1923, 1008 cm⁻¹ (oxidation state marker band). ¹H NMR (500 MHz, CD₂Cl₂): δ 3.08 (d, *J* = 6.8, 2 H), 5.87 (t, *J* = 7.3, 3 H), 6.42 (d, *J* = 7.50, 8 H), 6.53 (t, *J* = 7.07, 4 H), 6.59 (t, *J* = 1.85, 8 H), 6.69 (m, 32 H), 7.18 (d, *J* = 7.11, 4 H) and 7.42 (d, *J* = 6.94 Hz, 4 H). ¹³C NMR (75.6 MHz, CD₂Cl₂): δ 122.3, 124.9, 125.5, 125.8, 126.0, 126.2, 126.5, 126.9, 131.4, 132.1, 136.2, 138.4, 139.0, 144.7, 144.9 and 146.8. FAB mass spectrum: 1520 (*M*⁺), 1441 (*M*⁺ - py) and 1413 (*M*⁺ - py - CO) (Found: C, 75.4; H, 4.29; N, 3.70. Calc. for C₉₈H₆₅N₅OOS·2C₅H₅N: C, 76.7; H, 4.35; N, 3.80%).

[Os^{VI}(dpp)O₂] 4. To a dichloromethane solution (25 cm³) of [Os^{II}(dpp)(CO)(MeOH)] (50 mg, 0.037 mmol) was added *m*-chloroperoxybenzoic acid (100 mg, 0.058 mmol). A change from red to red-green occurred instantly, and the solution was stirred for 3 min. It was then concentrated by rotary evaporation to ca. 5 cm³, and chromatographed on a basic alumina column using dichloromethane as the eluent. The green band was collected; after solvent removal and subsequently recrystallization (CH₂Cl₂-MeCN) analytically pure complex **4** was obtained as dark green crystalline solids. Yield: 80%. IR(KBr): ν_{Os=O} 838, 1011 cm⁻¹ (oxidation state marker band). ¹H NMR (500 MHz, CDCl₃): δ 6.67 (m, 52 H) and 7.44 (d, *J* = 7.0 Hz, 8 H). FAB mass spectrum: 1446 (*M*⁺) (Found: C, 75.8; H, 4.31; N, 3.72. Calc. for C₉₂H₆₀N₄O₂Os: C, 76.2; H, 4.33; N, 3.76%).

X-Ray crystallography

X-Ray diffraction data were either collected on an Enraf-Nonius CAD-4 (for complexes **1** and **5**) or a Rigaku AFC7R (for **3**) four-circle diffractometer (graphite-monochromatised Mo-Kα radiation, λ = 0.7107 Å) using the θ-2θ scan mode at 298 K. The cell dimensions were obtained from a least-squares fit of 25 reflections in the range 11 < 2θ < 19.5° for **1** and 15.32 < 2θ < 30.12° for **5**. The data were corrected for Ψ-scan absorption. All the data reduction and structure refinement were performed using the NRCC-SDP-VAX packages or TEXSAN, SHELXL 93 programs.¹⁰ The structures were solved by the Patterson method and refined by least-squares cycles. All non-hydrogen atoms were refined with anisotropic thermal parameters, hydrogen atoms were included at idealised positions with a fixed isotropic thermal parameter U_H = U_C + 0.01 Å². Crystallographic data and experimental details for complexes **1**, **3** and **5** are summarised in Table 1.

CCDC reference number 186/952.

Stoichiometric oxidations of alkenes by [Ru^{VI}(dpp)O₂] and the isolation of [Ru^{IV}(dpp)(pz)₂]

To a degassed dichloromethane solution containing pyrazole (2% w/w) and alkenes (2 mmol) was added complex **2** (30 mg, 22 μmol) under argon. After stirring for 12 h the reaction mixture was filtered through a short column of neutral alumina with hexanes-ethyl acetate (9:1) as the eluent to remove the ruthenium complex. The organic products were then analysed and quantified, after addition of internal standards, by either GLC or ¹H NMR spectroscopy.

The ruthenium complex was then eluted by dichloromethane, after addition of acetonitrile led to the isolation of [Ru^{IV}(dpp)(pz)₂] **5** as a dark purple crystalline solid. Yield: 80%.

IR(KBr): 1006 cm^{-1} (oxidation state marker band). FAB mass spectrum: 1458 (M^+), 1390 ($M^+ - \text{pz}$) and 1322 ($M^+ - 2\text{pz}$) (Found: C, 79.90; H, 4.23; N, 7.57. Calc. for $\text{C}_{98}\text{H}_{66}\text{N}_8\text{Ru}$: C, 80.82; H, 4.45; N, 7.70%). μ_{eff} (Evans' method) = 3.24 μ_{B} .

Aerobic alkene oxidations catalysed by $[\text{Ru}^{\text{VI}}(\text{dpp})\text{O}_2]$

In a typical experiment complex **2** (15 mg, 11 μmol) was stirred with an excess of alkenes (2 mmol) in benzene–acetonitrile (9:1), 2 cm^3 under 1 atm oxygen for 4 h at 25 $^\circ\text{C}$. The crude reaction mixture was then passed through a short alumina column using hexanes–ethyl acetate (9:1) as the eluent to remove the ruthenium complex. The organic products were characterised and quantified by either GLC or ^1H NMR spectroscopy using internal standard methods.

Kinetic measurements

Dichloromethane was distilled over CaH_2 before use. Pyrazole (99%, Aldrich) was used as received. Styrene and norbornene (bicyclo[2.2.1]hept-2-ene) were purified using standard procedures. The rates of reduction of $[\text{Ru}^{\text{IV}}(\text{dpp})\text{O}_2]$ by alkenes were measured by monitoring the decrease of absorbance of the ruthenium complex at 450 nm. The reactions were carried out with $[\text{alkenes}] \gg [\text{Ru}^{\text{VI}}]$. Plots of $\ln|A_\infty - A_t|$ vs. time are linear over four half-lives. The pseudo-first-order rate constants (k_{obs}) were determined on the basis of a least-squares fit by relation (1) where A_∞ and A_t are the absorbance at the completion of the

$$\ln|A_\infty - A_t| = -k_{\text{obs}}t - \ln|A_\infty - A_0| \quad (1)$$

reaction and at time t respectively; A_∞ readings were obtained for at least four half-lives. Second-order rate constants (k_t) were determined from the slopes of plots of k_{obs} vs. alkene concentration.

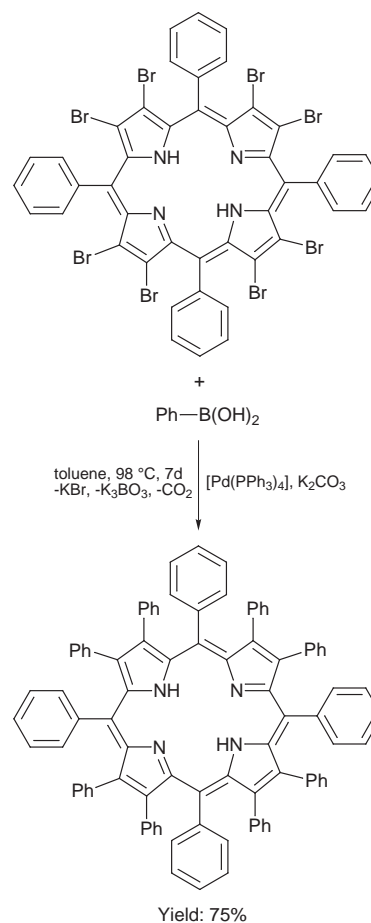
Results and Discussion

Synthesis and characterisation of $[\text{M}^{\text{VI}}(\text{dpp})\text{O}_2]$ ($M = \text{Ru}$ or Os)

2,3,5,7,8,10,12,13,15,17,18,20-Dodecaphenylporphyrin (H_2dpp) was prepared in good yield (75%) using the Suzuki cross-coupling reaction between phenylboronic acid and 2,3,7,8,12,13,17,18-octabromo-5,10,15,20-tetraphenylporphyrin, $[\text{H}_2\text{obtp}]$, as the principal step (Scheme 1).¹¹ The compound H_2obtp was derived from bromination of $[\text{Cu}^{\text{II}}(\text{tpp})]$ (yield = 76%), H_2tpp = 5,10,15,20-tetraphenylporphyrin, followed by demetallation using perchloric acid (yield = 91%).⁹ Compared with the procedure based on the condensation of benzaldehyde and 3,4-diphenylpyrrole (yield = 5.7%),¹² the strategy employing the Suzuki cross-coupling reaction is apparently more efficient and practical.

Insertion of Ru and Os into H_2dpp occurs readily upon treating $[\text{M}_3(\text{CO})_{12}]$ ($M = \text{Ru}$ or Os) with the free-base porphyrin in toluene (Ru) and diethylene glycol monomethyl ether (Os). The metal-carbonyl complexes $[\text{M}^{\text{II}}(\text{dpp})(\text{CO})(\text{MeOH})]$ were obtained after purification by column chromatography using alumina. Recrystallisation of the metal carbonyl complexes in a mixture of pyridine–dichloromethane–benzene led to quality crystals of $[\text{M}^{\text{II}}(\text{dpp})(\text{CO})(\text{py})]$ suitable for X-ray diffraction studies.

Complexes **1** (Fig. 1) and **3** are isostructural, and their porphyrin macrocycles exhibit both saddle and ruffle distortions. The edge-on-view of **1** (Fig. 2) shows that the pyrrole rings are alternately tilted up and down with respect to the least-squares plane of the 25-atom porphyrin core, and the phenyl rings are rotated into the macrocycle plane to minimise contact between the substituents. The saddle deformations in **1** and **3** are equally striking in that the pyrrole carbons experience an average displacement of 0.769 Å from the least-squares plane compared to 0.78 Å for free H_2dpp ¹³ and 0.99 for $[\text{Ni}^{\text{II}}(\text{dpp})]$.¹⁴ The angle



Scheme 1 Suzuki cross-coupling reaction

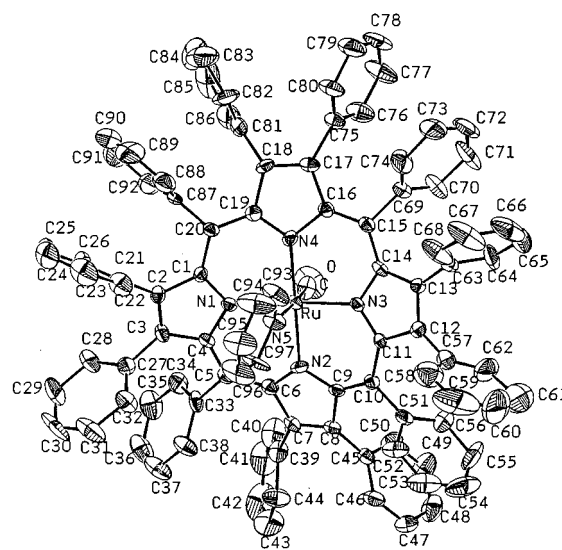


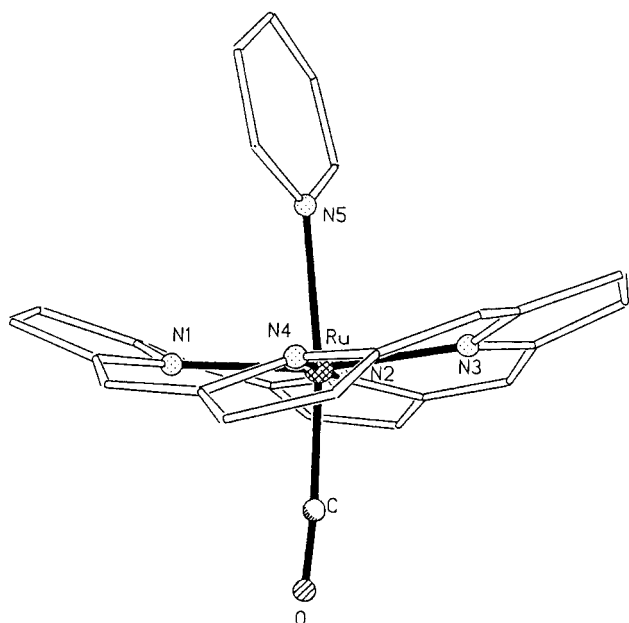
Fig. 1 Molecular structure of $[\text{Ru}^{\text{II}}(\text{dpp})(\text{CO})(\text{py})]$ with atom labelling scheme

between the least-squares planes of the pyrrole rings and that of the *meso* carbon atoms is 21 $^\circ$ for both complexes, and the Ru and Os atoms are displaced by 0.1006 and 0.0792 Å (Table 2) from the 25-atom porphyrin core respectively. The Ru–N (py) (2.240 Å) (Table 3) and the Os–N (py) (2.151 Å) bond distances fall within the range found in other pyridine-ligated metalloporphyrins.

Treatment of $[\text{M}(\text{dpp})(\text{CO})(\text{MeOH})]$ ($M = \text{Ru}$ or Os) complexes with *m*-chloroperoxybenzoic acid in CH_2Cl_2 –EtOH at room temperature afforded the saddle-distorted oxometalloporphyrins **2** and **4** in good yield. The $[\text{M}^{\text{VI}}(\text{dpp})\text{O}_2]$ complexes

Table 1 Crystallographic data and structure refinement for complexes **1**, **3** and **5**

	1	3	5
Empirical formula	C ₉₈ H ₆₅ N ₅ ORu·2C ₆ H ₆	C ₉₈ H ₆₅ N ₅ OOs·2C ₅ H ₅ N	C ₉₈ H ₆₆ N ₈ Ru·3CH ₃ CN·CH ₂ Cl ₂ ·7H ₂ O
Crystal size/mm	0.10 × 0.10 × 0.40	0.06 × 0.20 × 0.24	0.90 × 1.20 × 1.20
<i>M</i>	1585.92	1677.02	1791.0
Crystal symmetry	Triclinic	Triclinic	Orthorhombic
Space group	<i>P</i> $\bar{1}$ (no. 2)	<i>P</i> $\bar{1}$ (no. 2)	<i>Cmc</i> ₂₁ (no. 36)
<i>a</i> /Å	12.662(3)	12.673(3)	24.499(5)
<i>b</i> /Å	17.600(7)	17.649(4)	16.391(3)
<i>c</i> /Å	18.904(5)	18.937(4)	24.527(8)
<i>a</i> ^o	83.74(3)	84.08(3)	
<i>β</i> ^o	83.34(2)	83.52(3)	
<i>γ</i> ^o	85.94(3)	85.95(3)	
<i>U</i> /Å ³	4152.1(23)	4179(20)	9849(4)
<i>Z</i>	2	2	4
<i>D_c</i> /g cm ⁻³	1.269	1.333	1.208
<i>μ</i> /cm ⁻¹	2.372	15.78	3.911
No. measured reflections	10 816	15 231	4553
No. observed reflections [<i>I</i> > 2.0σ(<i>I</i>)]	5003	9651 [<i>I</i> > 6.0σ(<i>I</i>)]	2975
No. unique reflections	10 797	14 113	4553
<i>R_F</i>	0.069	0.078	0.063
<i>R'</i>	0.065	0.115	0.074
Goodness of fit	1.70	1.48	1.99

**Fig. 2** Edge-on-view of [Ru^{II}(dpp)(CO)(py)] (all phenyl groups are removed for clarity)

were isolated as air-stable solids. The presence of the weakly coordinating alcohol has proved crucial for the success of the synthesis; no complications such as dimerisation were observed. The absence of the CO stretch indicates the starting carbonyl complexes have been completely consumed. The dioxo-ruthenium(vi) and -osmium(vi) complexes show intense IR absorptions at 818 and 838 cm⁻¹ assigned to asymmetric O=Ru=O and O=Os=O stretches respectively, and the oxidation state marker bands at 1020 (Ru) and 1011 cm⁻¹ (Os) suggested that the ruthenium (**2**) and the osmium (**4**) centres are at +6 oxidation state.¹⁵

Magnetic susceptibility measurement established that complexes **2** and **4** are diamagnetic in accordance with a (d_{xy})² electronic ground state (here the O=M=O axis is taken as the *z* axis). The ¹H NMR spectra (298 K) of **2** and **4** show a broad doublet at δ 7.44 (*J* = 7.0 Hz, 8 H) assignable to the *ortho* protons at the *meso*-substituted phenyl rings and two sets of multiplets corresponding to the remaining 52 protons. The free H₂dpp is known to undergo two dynamic processes: NH tautomerism and

Table 2 Average out-of-plane displacements and dihedral angles between least-squares planes

	[Ru ^{II} (dpp)(CO)(py)]	[Ru ^{IV} (dpp)(pz) ₂]
Displacement (Å) ^a		
Ru	0.101	0.039
N ^{1,3}	+0.077	+0.066
N ^{2,4}	-0.0926	-0.068
C _α	±0.4561	
C _{α'}	±0.132	±0.379
C _β	±0.890	
C _{β'}	±0.649	±1.06
Dihedral angle ^o		
Pyrrole tilting ^b	20.93	27.78
Pyrrole phenyl twist ^c	75.50	66.95
<i>meso</i> -Phenyl twist ^d	66.48	47.21
Pyrrole planarity ^e	<0.05	<0.05

^a From the least-squares plane of the 25-atom porphyrin core.

^b Dihedral angle between the least-squares plane of a pyrrole ring and that of the four nitrogen atoms. ^c Dihedral angle between the least-squares planes of the pyrrole and phenyl rings. ^d Dihedral angle between the least-squares plane of a *meso*-phenyl ring and that of the *meso*-carbon atoms. ^e Largest deviation of any atoms in a pyrrole ring from the least-squares plane of the pyrrole ring.

macrocyclic inversion.^{12,13} Using variable-temperature NMR the activation free energy (ΔG^\ddagger) for the ring inversion process was estimated to be 10.9 kcal mol⁻¹. No dynamic processes were observed for **1–4** (ΔG^\ddagger < 7.0 kcal mol⁻¹), although the porphyrin ligand must be non-planar. Presumably, the macro-

cyclic inversion barriers for the ruthenium and osmium complexes are too low to be detected. The small inversion barrier is not inconceivable since the macrocyclic inversion barrier observed in the free H₂dpp porphyrin should arise from the repulsion between the NH protons.¹⁶

As H₂dpp adopts a non-planar conformation in solution, the macrocyclic distortion should have an effect on the UV/VIS absorption spectra of the ruthenium and osmium complexes. The absorption maxima for **1–4** and the analogous complexes with the essentially ‘planar’ tpp ligand are summarised in Table 4. The optical data show that the absorption maxima of the Soret bands and the Q bands for **1–4** are all red shifted compared with those of the complexes containing tpp. Theoretical calculations^{16,18} performed by other workers have indeed suggested that the distortion of the macrocycle would lead to a

Table 3 Selected bond distances (Å) and angles (°) for [Ru^{II}(dpp)(CO)(py)] and [Ru^{IV}(dpp)(pz)₂]

[Ru ^{II} (dpp)(CO)(py)]		[Ru ^{IV} (dpp)(pz) ₂]	
Ru–N(1)	2.048(7)	Ru–N(1)	2.042(11)
Ru–N(5)	2.240(8)	Ru–N(4)	2.022(13)
Ru–C	1.933(12)	Ru–N(5)	2.083(12)
N(1)–C(1)	1.363(10)	N(1)–C(2)	1.385(13)
C(1)–C(2)	1.464(12)	N(4)–N/C(47)	1.288(17)
C(2)–C(3)	1.338(13)	C(1)–C(1a)	1.386(23)
C(1)–C(20)	1.424(13)	C(1)–C(2)	1.422(16)
C(2)–C(21)	1.469(12)	C(1)–C(11)	1.565(15)
C(21)–C(22)	1.388(15)	C(11)–C(12)	1.501(18)
C(20)–C(87)	1.468(11)	C(2)–C(3)	1.342(15)
N(1)–Ru–N(2)	89.7(3)	N(1)–Ru–N(2)	91.6(6)
N(1)–Ru–N(3)	170.0(3)	N(1)–Ru–N(3)	173.9(6)
N(1)–Ru–N(5)	83.2(3)	N(1)–Ru–N(4)	86.6(9)
N(1)–Ru–C	90.9(3)	N(2)–Ru–N(4)	89.4(3)
N(2)–Ru–N(3)	89.7(3)	N(2)–Ru–N(2a)	176.5(7)
N(2)–Ru–N(4)	179.6(3)	N(2)–Ru–N(3)	88.5(6)
N(2)–Ru–N(5)	90.8(3)	N(2)–Ru–N(4)	89.4(3)
N(2)–Ru–C	87.5(4)	N(2)–Ru–N(5)	90.8(3)
N(3)–Ru–N(4)	90.4(3)	N(2a)–Ru–N(3)	88.5(6)
N(3)–Ru–N(5)	86.9(3)	N(2a)–Ru–N(4)	89.4(3)
N(3)–Ru–C	99.1(3)	N(2a)–Ru–N(5)	90.8(3)
N(4)–Ru–N(5)	88.8(3)	N(3)–Ru–N(4)	99.5(9)
N(4)–Ru–C	92.9(4)	N(3)–Ru–N(5)	86.1(11)
N(5)–Ru–C	173.8(3)	N(4)–Ru–N(5)	174.4(13)
Ru–C–O	173.8(10)	Ru–N(2)–C(4)	120.6(12)
C(1)–N(1)–C(4)	109.4(7)	C(4)–N(2)–C(7)	107.2(8)
N(1)–C(1)–C(2)	107.9(7)	Ru–N(4)–N/C(47)	126.4(10)
C(1)–C(2)–C(3)	106.0(7)	N/C(47)–N(4)–N/C(47a)	98.5(16)
C(1)–C(2)–C(21)	126.5(8)	N(2)–C(4)–C(5)	109.0(10)
C(3)–C(2)–C(21)	126.2(9)	C(4)–C(5)–C(23)	126.3(10)
N(1)–C(4)–C(5)	123.7(8)	C(6)–C(5)–C(23)	131.4(10)
C(4)–C(5)–C(6)	126.6(8)	C(5)–C(23)–C(3)	127.6(10)
C(4)–C(5)–C(33)	114.2(7)	C(5)–C(23)–C(24)	129.6(13)
C(27)–C(28)–C(29)	119.0(13)	C(24)–C(23)–C(28)	115.0(12)
		C(4)–C(3)–C(17)	117.4(9)

Table 4 The UV/VIS spectra data of non-planar ruthenium and osmium dpp complexes in CH₂Cl₂ at room temperature

Compound	λ/nm (log ε)	
	B bands	Q bands
H ₂ dpp	468 (5.38)	564 (4.13), 618 (4.15), 718 (4.01)
H ₂ tpp	416 (5.40)	514 (4.19), 548 (4.01), 589 (4.08), 645 (4.01)
[Ru ^{II} (dpp)(CO)(py)]	430 (5.26), 271 (4.82)	505 (sh) (4.56), 578 (4.38)
[Ru ^{II} (tpp)(CO)(py)]*	413 (5.45)	5.32 (4.25), 568 (3.57), 495 (sh) (3.71)
[Ru ^{VI} (dpp)O ₂]	448 (4.78), 358 (sh) (3.98)	550 (3.85), 586 (3.59)
[Ru ^{VI} (tpp)O ₂]	418 (5.29), 340 (sh) (4.19)	518 (4.24), 545 (sh) (3.89)
[Os ^{II} (dpp)(CO)(py)]	428 (5.03), 279 (4.68)	474 (sh) (4.44), 556 (4.10)
[Os ^{II} (tpp)(CO)(py)]	406 (4.45)	518 (4.23)
[Os ^{VI} (dpp)O ₂]	419 (4.68), 356 (4.27)	498 (sh) (4.23), 608 (3.89), 669 (sh) (3.67)
[Os ^{VI} (tpp)O ₂]	395 (4.82), 339 (4.15)	479 (sh) (4.08), 586 (3.71)
[Ru ^{IV} (dpp)(pz) ₂]	436 (5.24), 332 (4.71)	521 (4.66), 551 (4.21)

* Data taken from ref. 17.

large destabilisation of the ligand’s HOMOs together with a small destabilisation of the LUMOs, hence the smaller HOMO – LUMO gap results in the red shift of the optical spectra.

The electrochemical potentials of complexes **1–4** (0.1 M NBu₄PF₆–CH₂Cl₂) listed in Table 5 also reveal that the sterically induced macrocyclic distortion promotes oxidation by raising the HOMO energies. For instance, the cyclic voltammogram of [Ru^{VI}(dpp)O₂] in dichloromethane shows one quasi-reversible and one irreversible oxidation couple together with one irreversible reduction wave. With reference to previous studies,¹⁹ the quasi-reversible oxidation couple is tentatively assigned as the ligand-centred oxidation [Ru^{VI}(dpp)O₂] – e[–] → [Ru^{VI}(dpp⁺)O₂], E₁ = 0.55 V vs. ferrocenium–ferrocene. A noticeable drop in the magnitude of the oxidation potential of 240 mV due to the conformational distortion of the porphyrin ring is observed when compared with that of [Ru^{VI}(tpp)O₂] (E₁ = 0.79 V) (entry 3 vs. 4). A comparable drop in the oxidation potential (180 mV) is also noticed for the oxidation of [Os^{VI}(dpp)O₂] in dichloromethane when compared with the analogous tpp complex (entry 7 vs. 8). Since **1** and **3** are isostructural, we would anticipate that the dodecaphenylporphyrin ligand in **2** and **4** should exhibit similar degrees of conformational distortion; the HOMOs have experienced similar degrees of destabilisation vs. the analogous tpp complexes of Ru and Os.

Stoichiometric alkene oxidations by [Ru^{VI}(dpp)O₂]

The complex [Ru^{VI}(dpp)O₂] **2** is a competent oxidant of alkenes (Table 6), and as expected the analogous dioxoosmium(VI) complex **4** is unreactive towards organic oxidations. Stoichiometric oxidation of some representative alkenes such as nor-

Table 5 Electrochemical data (in V vs. ferrocenium–ferrocene) for the non-planar ruthenium and osmium dpp complexes

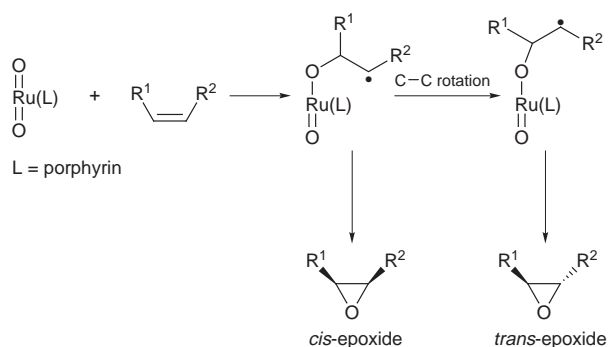
Entry	Compound	E ₁ ^{ox}		E ^{red a} III
		I	II	
1	[Ru ^{II} (dpp)(CO)(py)]	0.51 ^b	0.13 ^b	
2	[Ru ^{II} (tpp)(CO)(py)]	0.89 ^c	0.37 ^b	
3	[Ru ^{VI} (dpp)O ₂] ^d	0.90 ^a	0.55 ^c	–1.00
4	[Ru ^{VI} (tpp)O ₂] ^d	0.79 ^c		–0.83
5	[Os ^{II} (dpp)(CO)(py)]	0.74 ^b	0.11 ^b	
6	[Os ^{II} (tpp)(CO)(py)]	1.01 ^b	0.26 ^b	
7	[Os ^{VI} (dpp)O ₂] ^d	0.97 ^c	0.62 ^c	–1.20
8	[Os ^{VI} (tpp)O ₂]	0.80 ^c		–1.34
9	[Ru ^{IV} (dpp)(pz) ₂] ^d	0.78 ^c	0.45 ^b	–0.41

Conditions: in 0.1 mol dm^{–3} NBu₄PF₆ in CH₂Cl₂ using Ag–AgNO₃ in MeCN as the reference electrode and a glassy carbon working electrode; scan rate 100 mV s^{–1}. ^a Irreversible. ^b Reversible couple. ^c Quasi-reversible couple. ^d Solvent: CH₂Cl₂–MeCN (10:1).

Table 6 Stoichiometric oxidation of alkenes by $[\text{Ru}^{\text{VI}}(\text{dpp})\text{O}_2]$

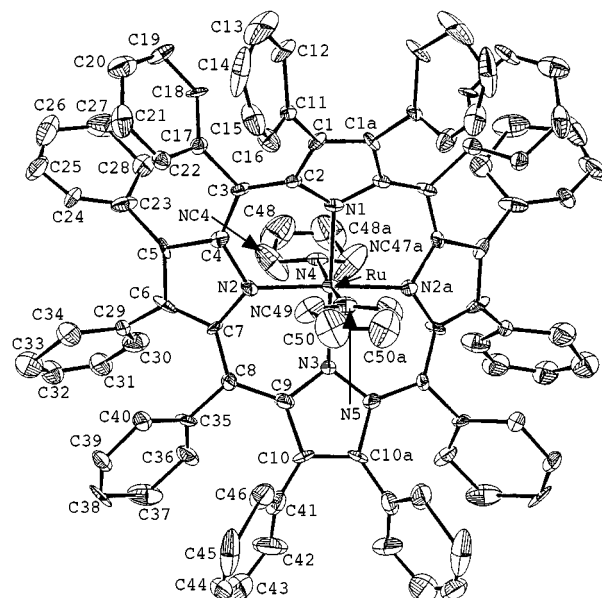
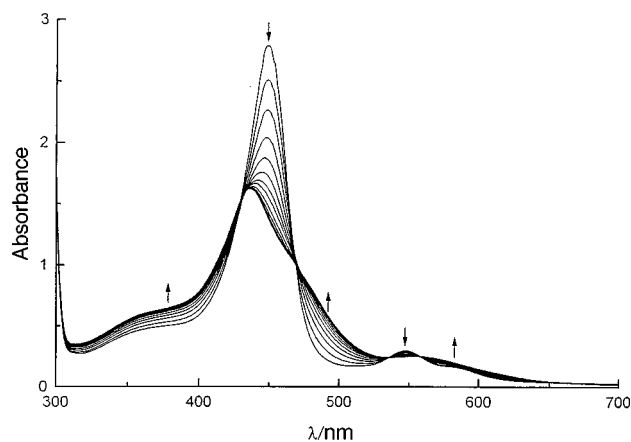
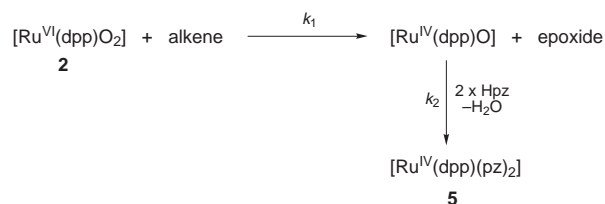
Entry	Alkene	Products	Yield (%) ^a
1	Norbornene	2,3- <i>exo</i> -Epoxynorbornane	>99 ^b
2	Styrene	Styrene oxide	>99 ^b
		Benzaldehyde	n.d. ^c
		Phenylacetaldehyde	n.d.
3	Cyclohexene	Cyclohexene oxide	14 ^b
		Cyclohex-2-en-1-ol	80 ^b
		Cyclohex-2-en-1-one	3 ^b
4	<i>cis</i> -Stilbene	<i>cis</i> -Stilbene oxide	>99 ^d
		<i>trans</i> -Stilbene oxide	n.d.
		Benzaldehyde	n.d.
5	<i>cis</i> - β -Methylstyrene	<i>cis</i> - β -Methylstyrene oxide	85 ^d
		<i>trans</i> - β -Methylstyrene oxide	14 ^d

^a Yield based on $[\text{Ru}^{\text{VI}}(\text{dpp})\text{O}_2]$. ^b Determined by gas chromatography. ^c n.d. = Not detected. ^d Determined by ¹H NMR spectroscopy using 1,1-diphenylethylene as the internal standard.



bornene (entry 1) and styrene (entry 2) in CH_2Cl_2 containing 2% (w/w) of pyrazole afforded almost quantitatively (>99%) *exo*-epoxynorbornane and styrene oxide respectively without C=C bond cleavages and rearrangement products. Allylic C-H oxidation prevailed when cyclohexane (entry 3) was used as the substrate; 80% of cyclohex-2-en-1-ol together with only 18% of cyclohexene oxide were formed. Oxidation of *cis*-stilbene was accompanied by full stereoretention giving rise to *cis*-stilbene oxide exclusively. However $[\text{Ru}^{\text{IV}}(\text{dpp})\text{O}_2]$ failed to react with *trans*-stilbene, *i.e.* no *trans*-stilbene oxide was detected. The preference of the dioxoruthenium(vi) complex for *cis*-alkene results from the unfavourable interaction of the phenyl rings of *trans*-stilbene with the porphyrin ligand, based on the 'side-on approach' model proposed first by Groves and co-workers.²⁰ The product stereoselectivity for the oxidation of *cis*-alkenes could be influenced by the steric bulkiness of the peripheral substituents of the porphyrin ring. For instance, the sterically less encumbered $[\text{Ru}^{\text{VI}}(\text{oep})\text{O}_2]$ ¹⁹ ($\text{H}_2\text{oep} = 2,3,7,8,12,13,17,18$ -octaethylporphyrin) reacts with *cis*-stilbene to afford a mixture of *cis*- (16%) and *trans*-stilbene oxide (44%). The predominant formation of *trans*-epoxide was explained by the formation of a carboradical intermediate, and the unhindered C-C bond rotation causes *cis* to *trans* isomerisation (Scheme 2).²¹ Indeed, reaction of **2** with *cis*-alkenes, which have smaller substituents such as *cis*- β -methylstyrene, produces a significant amount of *trans*-epoxide (14%) (entry 5).

For all oxidation reactions, $[\text{Ru}^{\text{IV}}(\text{dpp})(\text{pz})_2]$ **5** (pz = pyrazolate) was isolated as the final product and characterised by crystallographic means. The monomeric complex **5** has two axial pyrazolate ligands, and similar well characterised ruthenium(IV) porphyrin bis(amide) complexes have limited precedents in the literature. The oxidation marker band (IR spectroscopy) located at 1006 cm^{-1} is consistent with a ruthenium(IV) formulation.²¹ The complex is an air-stable and

**Fig. 3** Molecular structure of $[\text{Ru}^{\text{IV}}(\text{dpp})(\text{pz})_2]$ with atom labelling scheme**Fig. 4** The UV/VIS spectral trace for the reaction of $[\text{Ru}^{\text{VI}}(\text{dpp})\text{O}_2]$ ($1 \times 10^{-5}\text{ mol dm}^{-3}$) with styrene ($5 \times 10^{-2}\text{ mol dm}^{-3}$) in CH_2Cl_2 (2% pyrazole) in the range 300–700 nm**Scheme 3** $k_2 \gg k_1$

paramagnetic species, the μ_{eff} of $3.24\ \mu_{\text{B}}$ (by Evans' method in CHCl_3 -MeOH at room temperature) is slightly greater than the spin-only value ($2.83\ \mu_{\text{B}}$) required for two unpaired electrons. The crystal data, structural distortion parameters, bond distances and angles for **5** are summarized in Tables 1–3. The porphyrin macrocycle of **5** (Fig. 3) also exhibits out-of-plane distortions creating a saddle-shape structure similar to that found in **1** and **3**. The average Ru–N (pz) bond distances are found to be 2.022(13) and 2.083(12) Å, these values are comparable to 2.111(11) Å for Ru–N (pz) and 2.025(11) Å for Ru–N (amide) in $[\text{Ru}^{\text{IV}}(\text{tpp})(\text{pz})(\text{NH}\text{SO}_2\text{C}_6\text{H}_4\text{Me-}p)]$,^{22b} and the Ru–N (amide) distances of 1.987–2.044(5) Å found in $[\text{Ru}^{\text{IV}}(\text{chbae})(\text{PPh}_3)(\text{py})]$,²³ [chbae = 1,2-bis(3,5-dichloro-2-hydroxybenz-amido)ethane tetraanion]. The two pz ligands are *trans* to each other with the N (pz)–Ru–N (pz) bond angle of $174.4(13)^\circ$.

Table 7 Aerobic oxidation of alkenes catalysed by [Ru^{VI}(dpp)O₂]

Alkenes	Products	Turnover ^a
Norbornene	2,3- <i>exo</i> -Epoxynorbornane	40 ^b
Styrene	Styrene oxide	32 ^b
	Benzaldehyde	7 ^b
Cyclohexene	Phenylacetylaldehyde	Trace
	Cyclohexene oxide	8 ^b
	Cyclohex-2-en-1-ol	20 ^b
	Cyclohex-2-en-1-one	11 ^b
Cyclooctene	Cyclooctene oxide	24 ^b
	<i>cis</i> -Stilbene	10 ^c
<i>cis</i> -Stilbene	<i>trans</i> -Stilbene oxide	3 ^c
	Benzaldehyde	Trace

^a Based on the amount of [Ru^{VI}(dpp)O₂]. ^b Yield determined by gas chromatography using 1,4-dichlorobenzene as the internal standard. ^c Yield determined by ¹H NMR spectroscopy using 1,1-diphenylethylene as the internal standard.

Fig. 4 depicts the UV/VIS spectral change for the reaction of complex **2** with styrene in dichloromethane containing 2% pyrazole (Hpz). The observation of isosbestic points throughout the reaction indicates that the putative oxoruthenium(IV) intermediate should be at very low concentration compared to **2** and **5**. Scheme 3 is proposed for the oxidation reactions. Kinetic experiments revealed that the reactions of **2** with alkenes in dichloromethane (2% of Hpz) display clean first-order kinetics and the observed rate constants, k_{obs} , were determined by monitoring at 450 nm under pseudo-first-order conditions, *i.e.* [alkene] \gg [**2**]. A second-order rate law, $\text{rate} = k_1[\mathbf{2}][\text{alkene}]$, is established. With norbornene and styrene the second-order rate constants (k_1) in dichloromethane at 25.9 °C are $(3.79 \pm 0.04) \times 10^{-3}$ and $(4.78 \pm 0.09) \times 10^{-3} \text{ dm}^3 \text{ mol}^{-1} \text{ s}^{-1}$ respectively. These values are close to the second-order rate constants for the oxidation reactions of styrene $[(4.30 \pm 0.3) \times 10^{-3} \text{ dm}^3 \text{ mol}^{-1} \text{ s}^{-1}]$ and norbornene $[(3.01 \pm 0.09) \times 10^{-3} \text{ dm}^3 \text{ mol}^{-1} \text{ s}^{-1}]$ with the planar [Ru^{VI}(tpp)O₂] complex.²⁴ To account for the similar reactivities of the planar and saddle-distorted dioxoruthenium(VI) porphyrin complexes, we propose that the macrocyclic distortion should mainly destabilise the ligand's HOMO energies; however, the LUMOs related to the O=Ru=O moiety are relatively less perturbed, and therefore their electrophilicities would not differ significantly.²⁵

Catalytic aerobic alkene oxidations by [Ru^{VI}(dpp)O₂]

The complex [Ru^{VI}(dpp)O₂] can mediate alkene epoxidation with the use of molecular dioxygen (1 atm). In a typical experiment, **2** (15 mg, 11 μmol) was stirred with 2 mmol of alkenes in benzene–acetonitrile (9 : 1) at room temperature under dioxygen (1 atm) for 4 h. The reaction products were quantitatively analysed and identified by gas chromatography. A prolonged reaction for 12 to 24 h did not afford higher turnover. After 5 h of the reactions, traces of **2**, [Ru(dpp)(CO)] and some unidentified ruthenium complex were isolated.

When norbornene and cyclooctene were used as the substrates, the corresponding epoxides were the dominant products (Table 7). Allylic C–H oxidation is the major reaction undertaken by cyclohexene leading to cyclohex-2-en-1-ol and cyclohex-2-en-1-one, together with a minor production of cyclohexene oxide. Oxidation of styrene afforded a mixture of styrene oxide and benzaldehyde (C=C cleavage product) in a ratio of 4 : 1. The reaction of *cis*-stilbene under the oxidative conditions remains largely stereoretentive albeit with a small amount of *trans*-oxide formed.

When styrene and norbornene were used as the standard substrates [Ru^{VI}(tpp)O₂] and [Ru^{VI}(oep)O₂] attained <5 turnovers for the catalytic aerobic oxidation under identical reaction conditions. The formation of the catalytically inactive μ -oxo ruthenium dimers should be responsible for the catalyst

deactivation. Groves and Quinn^{19c} showed that the sterically encumbered [Ru^{VI}(tmp)O₂] (H₂tmp = 5,10,15,20-tetramesitylporphyrin) can avoid the μ -oxo dimer formation and give higher catalyst turnover in a range of 22–46 for oxidation of norbornene and *cis*- β -methylstyrene. In this work, the turnover number and selectivity of the Ru–dpp system are comparable to that of the Ru–tmp system. By examining the crystal structures of [Ru^{II}(dpp)(CO)(py)] and [Ru^{IV}(dpp)(pz)₂] complexes, the dioxoruthenium(VI) [Ru^{VI}(dpp)O₂] and [Ru^{VI}(tpp)O₂] complexes are anticipated to have similar steric environments, and hence their propensity to μ -oxo dimer formation under the catalytic conditions would be alike. The apparent increase in catalytic activity *vs.* [Ru^{VI}(tpp)O₂] and [Ru^{VI}(oep)O₂] could be due to the lower oxidation potential of **2** induced by the non-planar distortion of the porphyrin macrocycle.

Conclusion

Two highly distorted oxometalloporphyrin (Ru and Os) complexes of 2,3,5,7,8,10,12,13,15,17,18,20-dodecaphenylporphyrin have been synthesized based on the procedure previously developed for the preparation of [Ru^{VI}(por)O₂] with suitable modification. X-Ray analyses of [M^{II}(dpp)(CO)(py)], M = Ru or Os, and **5** revealed dpp exhibits both saddle and ruffle distortions. Metalloporphyrins **2** and **4** are believed to adopt similar conformational distortion based on the UV/VIS spectroscopic and electrochemical studies. Complex **2** is a competent oxidant for alkene epoxidation and shows an enhanced catalytic activity towards aerobic epoxidation when compared with [Ru^{VI}(tpp)O₂] and [Ru^{VI}(oep)O₂].

Acknowledgements

We acknowledge support from The University of Hong Kong and Hong Kong Research Grant Council.

References

- (a) J. L. Hoard, in *Porphyrins and Metalloporphyrins*, ed. K. M. Smith, Elsevier, Amsterdam, 1975, ch. 8; (b) W. R. Scheidt, in *The Porphyrins*, ed. D. Dolphin, Academic Press, New York, 1979, vol. 3, ch. 10; (c) W. R. Scheidt and Y. J. Lee, *Struct. Bonding (Berlin)*, 1987, **64**, 1; (d) K. M. Barkigia, L. Chantranupong, K. M. Smith and J. Fajer, *J. Am. Chem. Soc.*, 1988, **110**, 7566; (e) M. Ravikanth and T. K. Chandrashekar, *Struct. Bonding (Berlin)*, 1995, **82**, 105.
- J. Deisenhofer and H. Michel, *Science*, 1989, **245**, 1463.
- D. E. Tronrud, M. F. Schmid and B. W. Matthews, *J. Mol. Biol.*, 1986, **188**, 443.
- L. R. Furenliid, M. W. Renner and J. Fajer, *J. Am. Chem. Soc.*, 1990, **112**, 8987 and refs. therein.
- M. W. Grinstaff, M. G. Hill, J. A. Labinger and H. B. Gray, *Science*, 1994, **264**, 1311; J. A. Labinger, *Catal. Lett.*, 1994, **26**, 95.
- T. Shingaki, K. Miura, T. Higuchi, M. Hirobe and T. Nagano, *Chem. Commun.*, 1997, 861; Z. Gross and S. Ini, *J. Org. Chem.*, 1997, **62**, 5514; E. Galardon, P. Le Maux and G. Simonneaux, *Chem. Commun.*, 1997, 927.
- D. R. Coulson, *Inorg. Synth.*, 1972, **13**, 121.
- A. D. Alder, *J. Org. Chem.*, 1967, **32**, 476; P. Rothmund and A. R. Menotti, *J. Am. Chem. Soc.*, 1948, **70**, 1808.
- P. Bhyrappa and V. Krishnan, *Inorg. Chem.*, 1991, **30**, 239.
- TEXSAN-TEXRAY, Structure Analysis Package, Molecular Structure Corporation, Houston, TX, 1985; SHELXL 93, G. M. Sheldrick, University of Göttingen, 1993; NRCC-SDP-VAX, E. J. Cabe, Y. Le Page, J. P. Charland, F. L. Lee and P. S. White, *J. Appl. Crystallogr.*, 1989, **22**, 384.
- X. Zhou, Z. Y. Zhou, T. C. W. Mak and K. S. Chan, *J. Chem. Soc., Perkin Trans. 1*, 1994, 2519.
- C. J. Medforth and K. M. Smith, *Tetrahedron Lett.*, 1990, **31**, 5583.
- C. J. Medforth, M. O. Senge, K. M. Smith, L. D. Sparks and J. A. Shelnut, *J. Am. Chem. Soc.*, 1992, **114**, 9859.
- K. M. Barkigia, M. W. Renner, L. R. Furenliid, C. J. Medforth, K. M. Smith and J. Fajer, *J. Am. Chem. Soc.*, 1993, **115**, 3627.
- J. T. Groves and K.-H. Ahn, *Inorg. Chem.*, 1987, **26**, 3831.

- 16 C. J. Medforth, M. D. Berber, K. M. Smith and J. A. Shelnut, *Tetrahedron Lett.*, 1990, **31**, 3719.
- 17 J. J. Bonnet, S. S. Eaton, G. R. Eaton, R. H. Holm and J. A. Ibers, *J. Am. Chem. Soc.*, 1973, **95**, 2141.
- 18 T. Takeuchi, H. B. Gray and W. A. Goddard, III. *J. Am. Chem. Soc.*, 1994, **116**, 9730.
- 19 (a) W. H. Leung and C. M. Che, *J. Am. Chem. Soc.*, 1989, **111**, 8812; (b) J. T. Groves and R. Quinn, *Inorg. Chem.*, 1984, **23**, 3844; (c) J. T. Groves and R. Quinn, *J. Am. Chem. Soc.*, 1985, **107**, 5790.
- 20 J. T. Groves, *J. Chem. Educ.*, 1985, **62**, 928; J. T. Groves, Y. Hau and D. V. van Engen, *J. Chem. Soc., Chem. Commun.*, 1990, 436.
- 21 A. J. Castellino and T. C. Bruice, *J. Am. Chem. Soc.*, 1988, **110**, 158; J. T. Groves, K. H. Ahn and R. Quinn, *J. Am. Chem. Soc.*, 1988, **110**, 4217.
- 22 J. S. Huang, C. M. Che, Z. Y. Li and C. K. Poon, *Inorg. Chem.*, 1992, **31**, 1315; S. M. Au, W. H. Fung, M. C. Cheng, S. M. Peng and C. M. Che, *Chem. Commun.*, 1997, 1655.
- 23 C. M. Che, W. K. Cheng, W. H. Leung and T. C. W. Mak, *J. Chem. Soc., Chem. Commun.*, 1987, 418.
- 24 C. Ho, W. H. Leung and C. M. Che, *J. Chem. Soc., Dalton Trans.*, 1991, 2933.
- 25 H. Fujii, *J. Am. Chem. Soc.*, 1993, **115**, 4641.

Received 20th January 1998; Paper 8/00535D